Workflow for bio-guided fractionation of antimicrobial polyphenols from *Ugni molinae* leaves using microfractionation and centrifugal partition chromatography: *in vitro* and in *silico studies*.

EDGAR PASTENE[1,], MATIAS VENEGAS[1], KATHERINE FONSECA[2], APOLINARIA GARCÍA[2], FELIPE ZÚÑIGA[3],JULIO ALARCÓN[1], NANDIS FIALLOS[1], GIRLENNE CHRISTIANSEN[1], DIANA CORREA[1], LUIS BUSTAMANTE[4], AND MARCIA AVELLO[5].*

1. Laboratory of Synthesis and Natural Products, Department of Basic Sciences, Faculty of Sciences, University of Bío-Bío, Chillán, Chile.
2. Laboratory of Bacterial Pathogenicity, Department of Microbiology, Faculty of Biological Sciences, University of Concepcion, Concepcion, Chile.
3. Department of Clinical Chemistry and Immunology, Faculty of Pharmacy, University of Concepcion, Concepcion, Chile.
4. Department of Instrumental Analysis, Faculty of Pharmacy, University of Concepcion, Concepcion, Chile.
5. Laboratory of Pharmacognosy, Department of Pharmacy, Faculty of Pharmacy, University of Concepción, Concepcion, Chile.

ABSTRACT

The misuse of antibiotics has led to high levels of drug-resistance in specific pathogens, promoting the search of molecules from different natural sources or the design of novel drug candidates. Medicinal and edible plants are a rich source of bioactive compounds, in particular those of polyphenol class. In the present work, we screen the antimicrobial properties of an aqueous extract prepared from the leaves of Ugni molinae (Turz) against a panel of pathogenic bacteria strains formed by *Helicobacter pylori* (ATCC 43504), *Listeria monocytogenes* (ATCC 7644), *Staphylococcus aureus* (ATCC 9144), *Escherichia coli* (ATCC 11775), and *Salmonella enterica* (ATCC 13076). Preliminary fast HPLC-micro fractionation allows the identification of potential urease inhibitors using high throughput urea-phenol microplate assay. Afterwards, preparative fractionation by Centrifugal Partition Chromatography (CPC) allow to select the specific bioactive fractions.

A combination of antimicrobial tests, enzyme assays and molecular docking resulted in the identification by HPLC-MS/MS of two quercetin-O-(6′′-O-galloyl)-hexosides as the most dominant compounds in the active CPC-fractions. These bioactive compounds were quercetin-3-O-(6′′-O-galloyl)-8-galactopyranoside (hyperin 6”-gallate) and quercetin-3-O-β-D-(6′′-O-galloyl)-β-glucopyranoside (tellimoside). The molecular docking evaluation revealed that hyperin-6′′-gallate enter the binding site of urease and bind in through pi-cation, pi–pi, and H-bond interactions. In concordance with the in-silico assay, the CPC fraction containing this compound has the lowest values of IC50 for Jack bean (0.41 ± 0.08 µg/mL) and Helicobacter pylori (0.28 ± 0.08 µg/mL) ureases, respectively. Moreover, Label-Free Microscale Thermophoresis (MST) analysis suggest that this flavonoid forms a complex with urease, even inducing protein aggregation. In conclusion, Ugni molinae leaves has potent anti-urease flavonoids that can contribute to significantly reduce the acclimation of H. pylori in the acidic environmental of gastric mucosa.

Key words: *Ugni molinae, Centrifugal Partition Chromatography, Jack Bean urease, Helicobacter pylori, Microscale Thermophoresis, molecular docking.*

INTRODUCTION

Ugni molinae Turcz. (*U. molinae*) is a Chilean shrub belonging to the Myrtaceae family commonly called *“Murtilla”, “Murta”* or *“Uñi”*. It is distributed from the Maule region to the Island of Chiloé, including the Juan Fernández Archipelago [1]. The medicinal use of the plant is of indigenous origin and is based on the astringent properties of the leaves. Mapuche, Puelche and Pehuenche use infusions of the leaves in the treatment of diarrhea and dysentery [2].

Under field observation, *U. molinae* is a species that is not a regular target of pathogens, and this fact may be related to highly effective defense mechanisms that include secondary metabolites such as phenolic compounds and saponinic heterosides, which are not part of the defensive chains [3]. of the species, but that confer innate protection (Gudesblat 2007). The antimicrobial and insecticidal properties of plants are relevant in the defense of the plant itself and in the projection of an applicable use against pathogens in various areas. For example, in the search for new antimicrobial drugs, in the con-

***Author for correspondence:** *epastene@ubiobio.cl*

servation of various products and as allelochemicals. According to previous chemical results of *U. molinae* leaves, this species could have an innovative application in these areas.

Chemical composition of this plant is not yet completely clear; however, recent studies of the fruit and leaves indicate the presence of phenolic acids, flavonoids, anthocyanidins, tannins and saponinic heterosides [4]. Some of these compounds have recognized antioxidant, antidiabetic, and antimicrobial activities, although it has not been possible to identify all the molecules responsible for these effects and the underlying mechanisms [5–8]. Recently, two works reported that *U. molinae* phenolic-rich extracts help to avoid the aberrant aggregation of β-amyloid peptide (leaf extract) and polyglutamine-EGFP fusion proteins as model of Huntington`s disease in HEK-293 cells (berry extracts) [9,10].

However, despite the myriad of studies accumulated for this plant, it is likely that the relationship between the polyphenolic compounds present in its leaves and fruits does not reach relevant concentrations in the target tissues for which *in vitro* cellular models have generally been proposed [11–13]. In line with this statement, our group has focused on the gastrointestinal protective effects of these compounds and the result of their interaction with the intestinal biota [14–18].
As a result of this interplay, the intestinal microbiome can be modulated and can metabolize polyphenols with high molecular weight into more bioactive metabolites to improve their bioavailability [19]. In this way, the beneficial effects of plants rich in polyphenols could be related to their influence on the balance between pathogenic and non-pathogenic bacteria that reside in the intestinal tract. *U. molinae* flavonoids have reported in vitro gastrointestinal protective activity and is able to kill several pathogenic bacteria [7,8].

These properties could be due to not only the combined membranolytic effect of saponins, flavonoids and tannins, but also to more specific mechanisms such as, for example, the blocking of certain virulence factors or the ability to form biofilms in some bacteria [20]. One of the most complex bacteria to manage is *Helicobacter pylori*. Pharmacological treatment involves the use of a combination of antibiotics and antisecretory agents [21–23]. The goal of this aggressive therapy is its eradication. One of the characteristics of this bacteria is its great ability to survive in the acidic environment of the stomach and adhere efficiently to the gastric mucosa [24]. These features are related to the presence of enzymes such as urease and carbonic anhydrase, which allow it to buffer the surrounding environment [25].

In chronically infected individuals, *H. pylori* would constitute the main etiological agent of diseases such as chronic gastritis, peptic ulcer, adenocarcinoma, and gastric mucosa-associated lymphoma (MALT) [26–28]. On the other hand *Escherichia coli* is one of the bacteria best adapted to the human intestinal tract. Several phylogenetic groups have been described in human gut, but B2 and D groups seem to be associated with colorectal cancer (CRC), and adenomatous polyps [29].

These groups have high virulence and encode toxins such as cycle-inhibiting factor, cytolethal distending toxins, cytotoxic necrotizing factors and colibactin. These toxins are encoded in the polyketide synthase (pks) island and are responsible of cytotoxicity and malignant cell transformation and DNA damage [30]. L. monocytogenes is a Gram-positive facultative intracellular pathogen. Infection is frequent in individuals with lowered immunity such as transplanted patients or elderly people [31]. Since 1990, several studies have been conducted to monitor the presence of this bacteria in different food products in Chile. In one of this study, 77 samples of meat products, seafood and dairy products result positive for L. monocitogenes mainly in samples collected in Santiago. In 2000, the second stage of the study was carried out in salads ready-for-sale in different stores of Santiago. According to international scientific information, these products are the origin of large outbreaks of Listeriosis in humans.

From 709 samples analyzed, 26% of frozen salads and 10.5% fresh salads from supermarkets were positive. In Chile, L. monocytogenes is included in the regulation of notifiable diseases through laboratory vigilance. Recently in 2017, a new outbreak was reported in meat products. L. monocytogenes can adhere to gastrointestinal mucosa and form biofilms on different types of surfaces including plastic, stainless steel, and glass [32,33]. *Staphylococcus aureus* is a human pathogen that causes a variety of clinical infections, being a causal agent of bacteremia and infective endocarditis. This microorganism is also related to osteoarticular and skin infections. One of its characteristics is that it has several types of virulence factors and resistance to β-lactam antibiotics [34]. Methicillin-resistant *Staphylococcus aureus* (MRSA) has become a public health problem, which is why the World Health Organization (WHO) considers *S. aureus* MRSA as one of the clinical challenges that deserve to be investigated in collaborative way [35].

Therapeutic options are quite limited for the treatment of MRSA. Thus, vancomycin is the drug of choice for the management of complex infections due to MRSA. However, it has been reported that excessive use of vancomycin leads to the emergence of no susceptible strains [36]. Non-typhoid Salmonella enterica subspecies enterica serotypes are causative agents of foodborne infections in developed and developing countries. Salmonella enterica also is gain importance in public health since it is responsible for foodborne diseases (ETAS). Salmonella enterica is characterized by its high morbidity, the difficulty of controlling the sources of infection. As S. aureus MRSA, The World Health Organization (WHO) has recognized *S. enterica* in Latin America as an important agent behind salmonellosis [37]. This pathogen causes foodborne infection disease and is the major cause of diarrhea in humans. *S. enterica* not only infect humans, but also several animals like birds and cattle, generating important economic damage [38]. Like the other pathogens mentioned above, *S. enterica* is also of concern due to the development of multi-resistance. The above has motivated the search for natural agents for their elimination such as alkaloids, phenols, and terpenes [35].

The aim of the present work is to expand the existing data regarding bioactivities of an aqueous extract of *U. molinae* leaves, as well as identifying the compounds responsible for such properties. As far as we known, this is the first report that assess the anti-urease inhibitory potential of this plant.

Here in, our workflow considers the preliminary step of fast HPLC micro-fractionation coupled with microplate urease assay. Afterwards we used Centrifugal Partition Chromatography (CPC), as preparative anti-urease-assay-guided fractionation strategy to identify individual or clusters of small molecules followed by traditional dereplication approach by LC-MS/MS. Finally, molecular docking and Microscale Thermophoresis were used to corroborate the ligand-enzyme interactions.

EXPERIMENTAL

Vegetal material

Biological material from populations of *U. molinae* was collected in blooming season (November-march, 2008 – 2009) in the Biobío Region. Plant sample was identified by the taxonomist Dr. Roberto Rodríguez Oceanographic Sciences, University of Concepción. One sample of was deposited at the CONC herbarium (146511).

Preparation of Ugni molinae aqueous leaf extract (UMALE)

A sample of 100 g of Ugni molinae leaf powder, 500 mL of deionized water (80°C) was added, and the mixture was placed in water bath with stirring at 300 rpm overnight (40ºC). The mix was sonicated for 20 min and filtered. Finally, the extract was centrifuged at 4000 x g for 20 min and the supernatant divided in 5 Freeze Drying Flasks, deep frozen at -80ºC and lyophilized at ⁻50°C.

Antimicrobial Activity of UMALE Extract

For susceptibility tests, Columbia agar plates supplemented with 5% defibrinated horse blood were used, which were seeded with bacterial suspension standardized according to Mc Farland No. 2 ($6x10^8$ cfu/mL) of strains ATCC 43504 and J99 of *H. pylori*. The agar-well diffusion method using Mueller–Hinton (MH) medium was used to test the UMH and MH LLEs against *H. pylori* based on standard 2 of McFarland's turbidity. An inoculum of *H. pylori* was seeded onto the surface of the M-H-containing agar using a sterile cotton swab. The agar wells were then drilled using a sterile 6 mm drill and filled with 100 µL of each extract. Three dilutions of *U. molinae* was deposited.

Some wells were filled with 10% dimethylsulfoxide (DMSO) as a negative control. All plates were refrigerated at 4 °C for 30 min to allow the samples to spread before the growth of *H. pylori* began. The plates containing the inoculums were incubated in a GasPak™ anaerobic system "Oxoid" under suitable conditions, including a microaerobic environment at 37°C, and an incubation time of 72 h. The zones of inhibition that appeared were then measured in millimeters.

For L. monocytogenes ATCC 7644, *E. coli* ATCC 11775, *S. aureus* ATCC 9144, and S. enterica ATCC 13076, inoculum was spread using sterile swab on MRS agar plates, PALCAM and Müeller-Hinton, accordingly. Subsequently, Kirby-Bauer disc diffusion test was performed for UMAE sample. Plates were incubated for 24 h at 37°C under aerobiosis conditions. Antibacterial activity was tested at concentrations from 1 mg - 0.25 mg per sisk or well. In the well-diffusion assay (*H. pylori*), amoxicillin (AMX) (Sigma-Aldrich®) was used as antibiotic control at a concentration of 5 µg per well, and DMSO 20% and sterile distilled water were used as negative controls.

Table 1. Results of antimicrobial susceptibility tests for UMAE.

Strains	Inhibition zone (Mean ± SD, mm)					
	1 mg	0.5 mg	0.25 mg	AMX*	CC**	GE**
H. pylori 43504	31.0 ± 1.1[b]	20.5 ± 0.9[c]	12.8 ± 2.2[d]	23.7 ± 1.7	Not determined	Not determined
H. pylori J99	No activity was observed[a]	No activity was observed[a]	No activity was observed[a]	20.7 ± 0.6	Not determined	Not determined
S. enterica 13076	12.0 ± 1.5[a]	10 ± 0.7[a]	6.1 ± 1.1[b]	26.3 ± 1.5	25.0 ± 1.0	25.0 ± 0.3
L. monocytogenes 7644	12.1 ± 1.0[b]	9.3 ± 1.3[c]	6.0 ± 1.6[d]	15.0 ± 1.0	38.1 ± 0.8	38.2 ± 1.7
E. coli 11775	16.0 ± 2.1[b]	12.2 ± 1.8[c]	6.0 ± 1.2[d]	No activity was observed	27.2 ± 2.8	35.2 ± 3.0
S. aureus 9144	18.2 ± 1.8[b]	15.3 ± 0.8[c]	12.1 ± 2.1[d]	No activity was observed	25.8 ± 0.9	22.1± 2.1

*In *H. pylori* test, the analyzed concentration for AMX was 100 µg /mL (5 µg/well). **For other bacteria test, disks of gentamicin (GEN) 10 µg; chloramphenicol (CFN) 30 µg and amoxicillin (AMX) 30 µg were used. 2 UMAE was tested at 1 – 0.25 mg/well or disc. Values with different letter are significantly different for the same concentration of UMAE ($p \leq 0.05$).
Statistical analysis was made with ANOVA followed by Tukey´s test.

For Kirby Bauer test, control antibiotic susceptibility disks of amoxicillin 30 µg, gentamicin 10 µg, and chloramphenicol 30 µg were used. All tests were performed in triplicate and the observed antibacterial activity was expressed as the average of the inhibition diameters (mm) produced by the tested samples.

Micro-fractionation and preliminary anti-urease *in vitro* bioassay

Rapid microfractionation of UMAE was performed using a YL9111S binary pump coupled to the YL9120s UV/Vis detector (Young Lin®, Korea). Chromatography system was equipped with a 100 - 2.5 µm-C18, 4.6 mm x 100 mm Kromasil KR100 column (Eka Chemicals AB, Bohus, Sweden. The solvent system was composed of solvent A (ultrapure water containing 0.1 % formic acid, v/v) and solvent B (100% ACN). The gradient program was 0-5 min (0-3% B); 3-22 min (3-20% B); 22-24 min (20% B); 24-26 min (20-0% B); 26-30 min (0%B).

Finally, the column was re-equilibrated or additional 2 min. The flow rate was 0.5 mL/min, and the injection volume was 50 µL. Detection was performed by using UV-VIS chromatograms acquired at 280 nm. Eighty-two (82) fractions starting from 2.50 min were collected on a fraction collector 100CHF 100SA Advantec at 20 seconds interval, into deep well plates 96 well.

Plates were dried under vacuum at 40°C for 24 h. To eliminate any trace of organic solvent and formic acid, a stream of nitrogen gas was applied to the plate during 20 min. The dried microfractions were dissolved in 5 µL of DMSO and then diluted with 95 µL of urease buffer with substrate. Finally, 10 µL of urease was aliquoted to each well and the microplate was agitated and read after 30 min.

CPC apparatus and separation procedures

For the bio-guided fractionation of anti-urease compounds present in UMAE leaves, a CPC 250-L centrifugal partition chromatograph (Gilson, France) with a 250 mL total cell volume was used. The system has four-way switching valve to optional operation in descending or ascending modes. The CPC module was connected to PLC-2050 system (Gilson, France), with integrated UV detector and fraction collector. UMAE CPC fractionation was performed with two-phase solvent system composed of MtBE-BuOH-ACN-H_2O with 0.001%TFA at 4:2:3:8 v/v ratio [39].

The solvent mixture was automatically generated by the PLC-2050 equipment. The CPC rotor was first filled with 1.5 column volumes using the lower phase at 30 mL/min and 500 rpm rotation. Upper phase was pumped into the system in the ascending mode at a flow rate of 6 mL/min (780 psi) and rotational speed was increased from 0 to 1800 rpm.

After equilibrium, 1.5 g of UMAE sample was dissolved in 10 mL 1:1 mixture of upper and lower layers and injected into the CPC systems through the automatic port. Elution step was carried out for 150 min and then extrusion step was performed with stationary phase (lower) at 30 mL/min for additional 10 min to recover highly retained compounds. Elution was monitored using scan 200-600; 280 and 360 nm wavelengths, collecting fractions in 25 mL tubes. Fractions with similar composition were reunited according with on-line UV spectra and HPLC.

Urease inhibition assay

The inhibition of urease activity was performed according to the method of Tanaka et al (2004) with some modifications. The

Figure 1. HPLC microfractionation of *U. molinae* aqueous extract (UMAE). Red circles represent absence of anti-urease (Jack bean), activity and orange-yellow circles represent the presence of peaks with inhibitory activity.

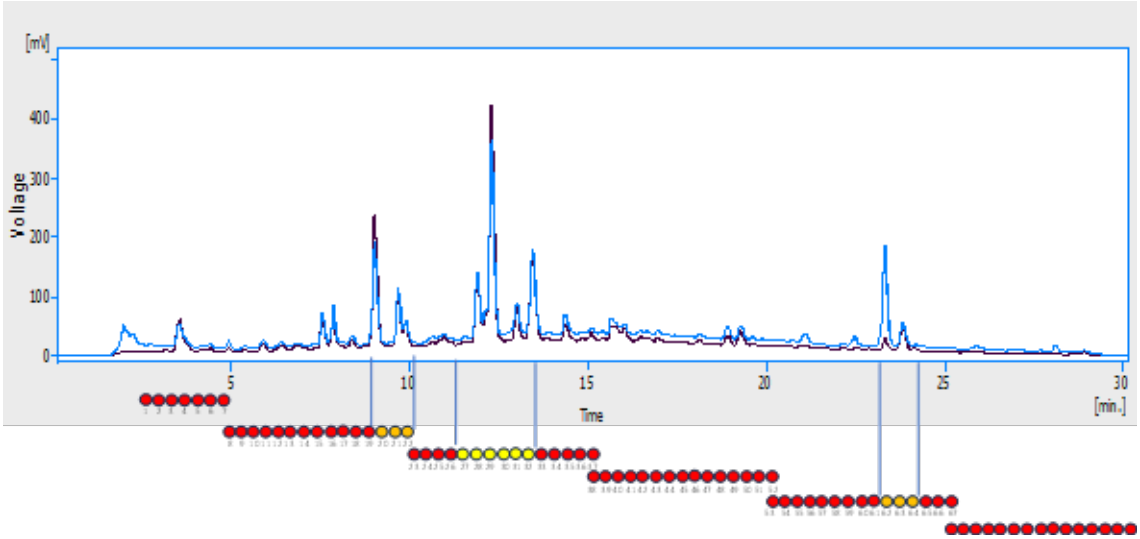

Figure 2. Preparative CPC fractionation of *U. molinae* aqueous extract (UMAE) in ascending mode.
Red rectangles represent zones without anti-urease activity and orange-yellow rectangles represent the presence of tubes with strong inhibition of Jack bean urease activity ($p \leq 0.05$ *versus* blank without enzyme).

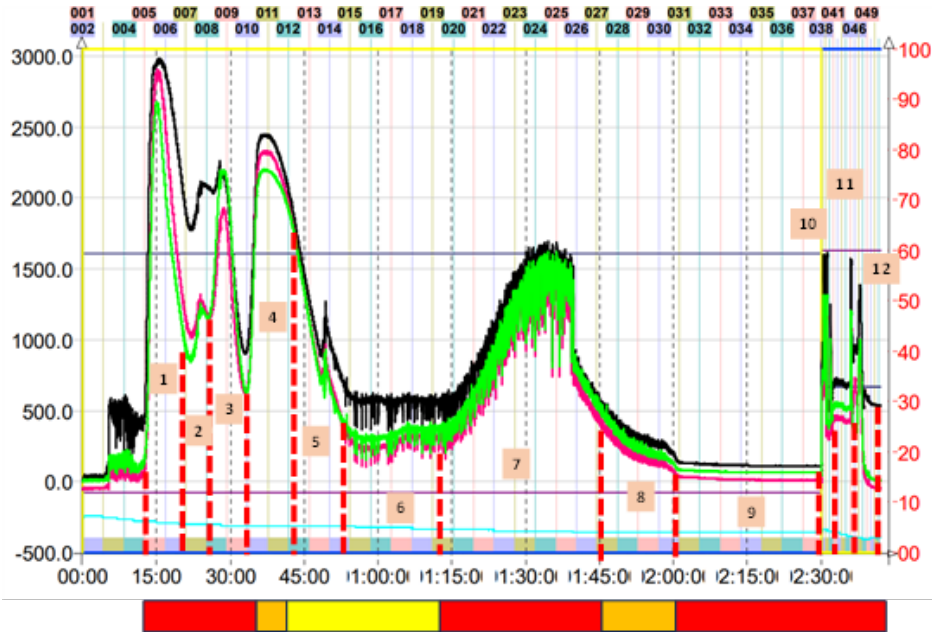

urea-phenol red substrate solution consisted of a mixture of 100 mM phosphate buffer at pH 6.8, 150 mM urea, and 0.002% phenol red. Urease from Canavalia ensiformis (Jack bean, Sigma-Aldrich, E.3.5.1.5) and *H. pylori* were used. Extraction of *H. pylori urease* was performed according to our previous works [40–42].

In 96-well plates, 10 µL of ureases, 10 µL of extract (inhibitor) were added, incubated for 30 minutes and subsequently 100 µL of the urea-phenol red substrate was added. Urease inhibition was evaluated using different concentrations of the *U. molinae* fractions. A plate reader was used to follow the progress of inhibition at 570 nm. The results were graphed for each extract with its corresponding percentage of inhibition at the different concentrations and the IC50 value (concentration that produce 50% of enzyme inhibition) was calculated.

LC-MS/MS analysis

HPLC-DAD-ESI-MS analysis of the CPC bio-active fractions was carried out in a Nexera UHPLC System (Shimadzu, Japan) coupled to a 3200 QTRAP Mass spectrometer (ABSCIEX, USA, MA). The separations were performed with a C18 core-shell column (Kinetex 150×4.6 mm, 2.6 µm) with a C18 UHPLC guard column (4.6 mm, 2.6 µm) (Phenomenex, USA, CA). The mobile phases were 0.1% formic acid in water (A) and acetonitrile (B), with a flow rate of 0.5 mL/min. The gradient of mobile phase B was from 15 to 20% in 1.5 min, then isocratically to 20% for 5.5 min, from 20 to 50 in 6 min, and 100% for 3 min followed by stabilization for 6 min to 15 % B. The MS/MS detection of phenolic compounds was carried out under the following previously optimized conditions: electrospray negative ionization mode, ⁻5 V collision energy, ⁻4000 V ioni-zation voltage, and capillary temperature at 450°C. Nitrogen was used as nebulizing gas (40 psi) and drying gas (50 psi).

Docking upon urease

Molecular docking was performed using the crystallized structure of urease from Jack Bean (4H9M; *https://doi.org/10.2210/pdb4H9M/pdb*), which was obtained from the RCSB Protein Data Bank. Crystallized ligands and water molecules were removed from the protein using Discovery Studio Visualizer v21.1.0.202998 software. On the other hand, the quercetin-3-O-(6′′-O-galloyl)-β-galactopyranoside ligand was recreated using ChemDraw Professional 16.0 software (PerkinElmer®). Avogadro v1.2.0 software was used to decrease the conformational energy of the ligand using the MMFF94 force field, optimal for organic compounds.

Finally, ligand-protein interactions were performed in MGLTools v1.5.7, where Kollman charges for the protein and Gasteiger charges for the ligand were added, adding polar hydrogens and binding non-polar hydrogens for both. The grid size was 80 Å (x,y,z) and placed on amino acids of interest (Arg 439, Ala 440, Thr 441, KCX 490, CME 592, His 593, Arg 609, Asp 633, Gln 635 and Met 637). The Lamarckian genetic algorithm was used to define the top 10 positions out of the 250,000 total. The interaction complexes were visualized in Discovery Studio Visualizer.

MST experimental procedure

All MST measurements were conducted on a NanoTemper Monolith NT. Label-free instrument (Müenchen, Germany), using Monolith NT. Premium Label-free coated zero background capillaries. Laser potency was automatically adjusted to 20%

in medium power. Ligan and protein concentrations for stock solution that will be used in pre-test (binding check) were 30 µM and 15 µM. For binding check, 20 µL of target and ligand stock solutions were diluted with 20 µL of phosphate saline buffer (PBS 1X). From these diluted samples, 20 µL each were mixed vortexing twice for 5 s. To reduce interaction with capillaries, 0.05% Pluronic F127 (Sigma-Aldrich, St. Louis, MO) was included in all samples. To eliminate particles, samples were centrifuged for 2 min at 120.000 rpm. Capillaries with target alone, protein, PBS and protein-ligand were disposed in the tray in triplicates [43].

Statistical analysis

Data were analyzed using the GraphPad Prism 4 statistical software. Values represent the means of at least three independent experiments, each conducted in quadruplicate. Data were analyzed by analysis of variance with post hoc comparison using Tukey's test.

RESULTS AND DISCUSSION

Antimicrobial Activity of UMALE Extract

The effectiveness of UMAE was evaluated on Gram positive and negative strains (Table 1). Bacterial susceptibility tests were carried out in agar plates and using a final concentration of 1 – 0.5 mg per well or disc.

According to the results presented in Table 1, UMAE show antibacterial activity against *H. pylori* ATCC 43504 but not activity was observed upon J99 strain. Although both strains are similar, their behavior against antibiotics is different. Therefore, this difference between strains may be due to several factors, and it can be theorized that UMAE bioactive compounds have a target-dependent mechanism that is expressed differently in each strain. For example, the MIC for tetracycline of J99 is almost 5 times higher than that reported for strain ATCC 43504 [44].

The reasons for resistance to this type of antibiotics range from different the expression of proteins called tetracycline-specific efflux pumps, which are members of the major facilitator superfamily (MFS) of transporters. Furthermore, since several bacteria have multiple rRNA copies, target-based mutations in rRNA explain this tetracycline resistance. This situation is usually seen in bacteria with low rRNA gene copy numbers. Hence, these mutations in 16S rRNA have been reported in *H. pylori* (1–2 16S rRNA copies) [45].

In a previous study carried out with *Gunnera tictoria polyphenols*, the sensitivity of both strains was similar, which is confirmed by what was stated above [39]. Despite this, the inhibition zones on the *H. pylori* ATCC 43504 strain are considerable and suggest a concentration-dependent effect. In general, UMAE has a moderate effect on the other strains investigated, where the results on *E. coli* and *S. aureus* stand out.

Micro-fractionation and preliminary anti-urease *in vitro* bioassay

The integration of HPLC micro-fractionation and bio-guided assay for fast identification of potential active compounds enable the systematic separation of extracts from a natural product. Moreover, these micro-separation techniques allow the coupling with different bioassays in parallel with sophisticated detection methods used for rapid dereplication of extracts. Therefore, this approach seeks lowering costs, saving time and resources for the isolation of novel drug candidates [46–48]. Figure 1 shows a representative chromatogram of the HPLC microfractionation of the aqueous extract of Ugni molinae (UMAE). The injection of 50 µL of a solution of the extract prepared at a concentration of 10 mg/mL was sufficient to preliminarily detect those peaks suspected of having anti-urease activity.

Only Jack bean urease was used because it has a declared activity and its cost is very low compared to *H. pylori* urease, which is reserved for testing the fractions subsequently obtained by CPC. In any case, both ureases have almost superimposable catalytic sites and therefore, normally a Jack bean urease inhibitor also tends to inhibit the bacterial enzyme [49].

As can be seen, after incubating the wells corresponding to t_R = 8 - 14 and 23 min, there was no development of purple color,

Figure 3. HPLC-DAD (360 nm) of enriched anti-urease CPC fractions of UMAE (5 and 6) using C18 core-shell column.

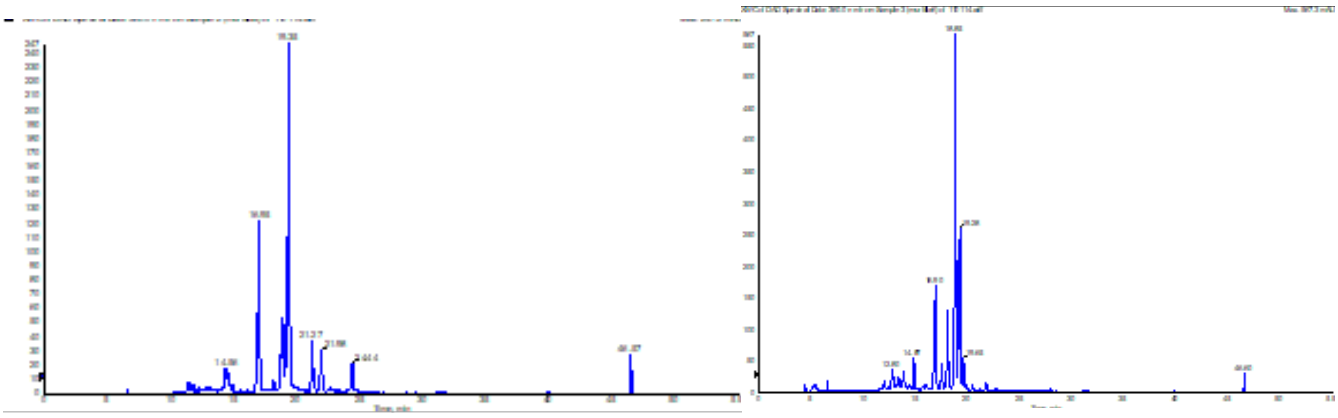

Table 2. IC_{50} values for CPC fractions with inhibitory activity upon jack bean urease.

Fraction Nº	IC_{50} (mg/mL) *
4	1,52 ± 0,11
5	0,41 ± 0,08
6	2,36 ± 0,07
7	8,28 ± 0,15
8	2,71 ± 0,04
9	1,57 ± 0,17
Acetohydroxamic Acid in µg/mL (AHA)	4.81 ± 0,05

*Urease inhibitory activity was determined after 30 min of preincubation with the CPC fractions.

Table 3. IC_{50} values for CPC fractions with inhibitory activity upon *H. pylori* urease.

Fraction Nº	IC_{50} (mg/mL) *
4	2,11 ± 0,10
5	0,28 ± 0,08
6	3,88 ± 0,11
7	7,93 ± 0,13
8	4,79 ± 0,08
9	3,29 ± 0,09
Acetohydroxamic Acid in µg/mL (AHA)	5.01 ± 0,12

*Urease inhibitory activity was determined after 30 min of preincubation with the CPC fractions.

which indicates an inhibition of urease due to the reduction in ammonia production. Phenol red remains yellow in those wells where there are potential inhibitors of the enzyme. It is important to note that this method has limitations that must be individualized. First, the type of inhibitor cannot be directly determined, for example whether it is competitive, non-competitive, reversible, irreversible, or mixed. If a very acidic substance elutes, it could affect the result of the reaction in the medium with phenol red. Finally, since the amounts injected are limited by the column load capacity and the threshold of the analytical detector, it is possible that some inhibitors remain undetected or that others could be overestimated. Some of these limitations can be overcome by using the alternative assay to measure urease activity.

Thus, determinations by the phenol-hypochlorite urease assay based on the measurement of the amount of ammonia released from urea can be used. However, this assay is more indirect and requires calibration with ammonium and removing aliquots from each well to stop the reaction [50]. In general, phenol red test is very useful and allows you to save resources and obtain additional information. For example, the elution time gives an idea of the polarity of the compounds and the same HPLC method can be used to select the solvent system in which the compounds of interest could be fractionated by CPC.
In fact, the peak area ratio between the signals of the bioactive compounds between 8-14 min present in the upper and lower phase of the MtBE-BuOH-ACN-H_2O system (with 0.001%TFA), it yields Kd values between 1.18-1.72, which is considered within the *"sweet spot"*, recommended for counter-current separations [51,52].

CPC separation of UMAE and anti-urease activity

Figure 2 shows a representative image of the preparative separation of the UMAE extract. The separation was carried out in ascending mode, which is equivalent to a separation in normal mode, that is, the nonpolar compounds elute first, while the more polar compounds are obtained in the extrusion stage, starting at 2:30 hours. Using the symmetry of the peaks and the similarity of the UV-VIS spectra obtained in the DAD detector as criteria to combine tubes, 12 fractions were generated, which were concentrated under vacuum and evaporated to subsequently evaluate their anti-urease activity.

As seen in the lower panel of Figure 2, fractions 5 and 6 (to a lesser extent 4 and 8), concentrate the compounds with the highest anti-urease activity and therefore, efforts will be concentrated on such fractions to elucidate that type of compounds underlying them. The IC_{50} values of each fraction are displayed in Table 2 and Table 3. Only those zones of CPC with significant ($p \leq 0.05$), activity over blank (without enzyme) were used to assess its anti-urease activity, since amount of *H. pylori* urease is limited and more expensive.

Figure 4. HPLC-ESI-MS/MS of main compound in fraction 5 from CPC. Upper panel showing the enhance mass spectrum for peak at tR = 17.036 min that presented a pseudomolecular ion at 615.5 m/z. Lower panel showing the ESI-MS/MS of the compound as enhanced product ions spectrum (EPI).

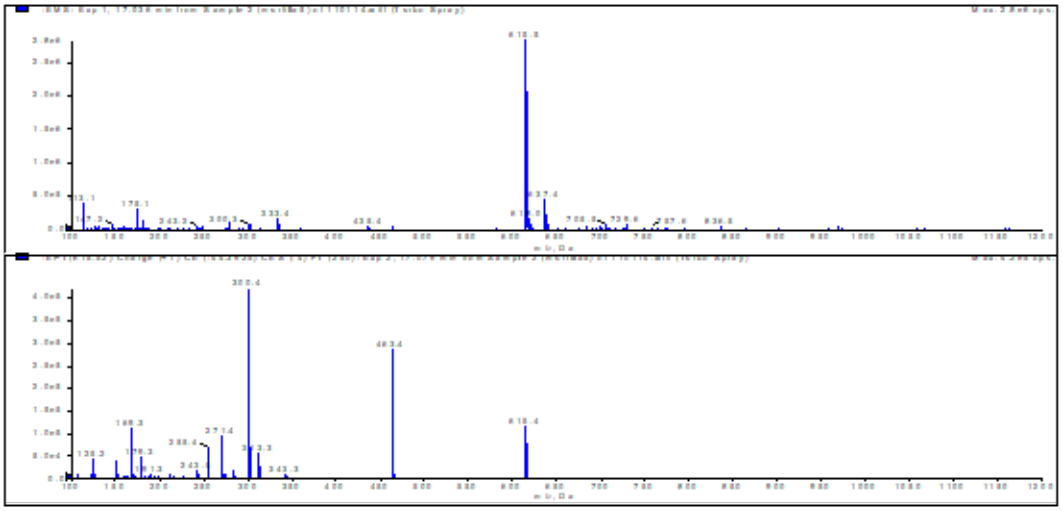

Figure 5. HPLC-ESI-MS/MS of main compound in fraction 6 from CPC. Upper panels showing the enhance mass spectrum for peaks at tR = 16.99 and 17.66 min that presented a pseudomolecular ion at 615.5 m/z. Lower panel showing the ESI-MS/MS of both compounds as enhanced product ions spectrum (EPI).

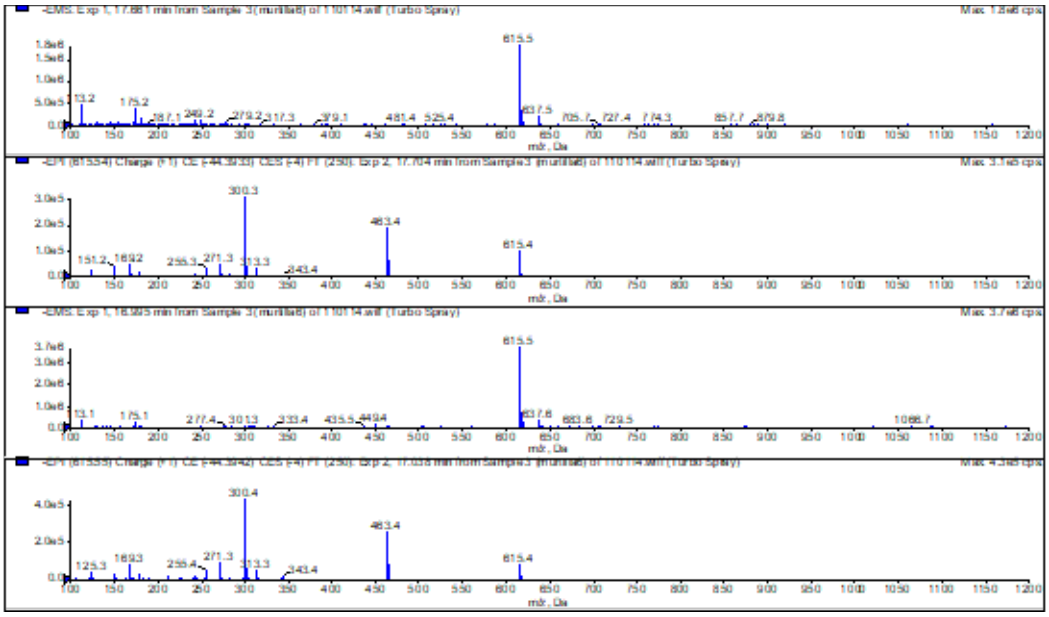

LC-MS/MS analysis

Figure 3 shows the plot of fractions 5 and 6 obtained in a chromatographic system with better resolution, equipped with a core-shell column. The signals suggest that there is some overlap between both fractions 5 and 6 and, therefore they could group together compounds of similar chemical nature. In fact, the analysis of the mass spectra of the predominant peaks indicates that at least the compound at t_R = 19.35 min is present in both fractions, although in a different proportion.

This compound is concentrated more in fraction 5, while the compound at t_R = 18.85 min is concentrated in fraction 6. It is important to note that the HPLC analysis is performed in a C-18 reverse phase and, therefore, the polarity is inverse in relation to what is observed in CPC. Compounds in fractions 5 and 6 showed three peaks between t_R = 17 - 20 min, with the molecular ions at m/z 615 and the same fragmentation pattern with ions at

Figure 6. 2-D interaction plots diagram of protein–ligand interaction depicting H bond and hydrophobic interactions between Quercetin 3-O-(6''-galloyl)-β-D-galactopyranoside against Jack bean urease.

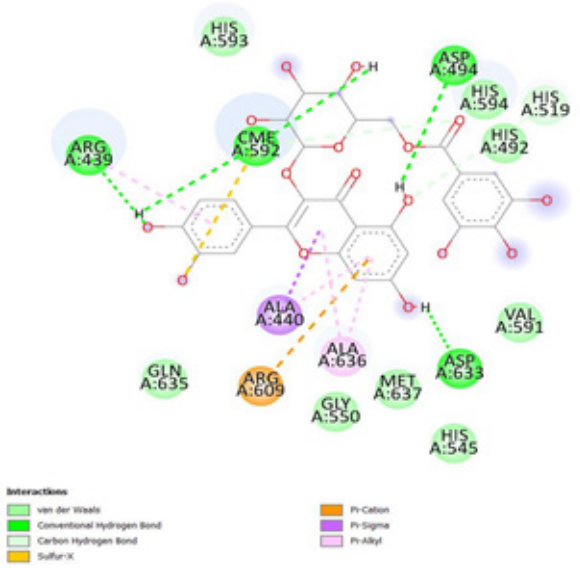

m/z 463, 300, and 169. Fragment corresponding to quercetin in at m/z 300 [M–H]- and the quercetin glucoside at m/z 463 [M–H]- are evident. The presence of a galloyl unit was evidenced by the neutral loss of 152 Da from the base peak at m/z 615. According with the elution order we proposed that these compounds are quercetin-O-(6-O-galloyl)-hexosides [4].

Thereby, tentatively the compound at t_R = 18.85 min was assigned as quercetin-3-O-β-D-(6′′-O-galloyl)-glucopyranoside and compound t_R = 19.35 min was assigned as quercetin-3-O-β-D-(6′′-O-galloyl)-galactopyranoside. The presence of both compounds was reported previously by Torres and coworkers [8] in an aqueous extracts of *U. molinae*. Peak at t_R = 16.995 min also showed a molecular ion at m/z 615 and MS/MS fragments at m/z 463, resulting from the loss of a galloyl group from [M – H] −, and at m/z 301, resulting from the loss of one hexose unit (162 Da). However, the UV spectra of this compound don't correspond with the typical UV-VIS trace of flavonoids and resemble better an ellagic acid derivative. Therefore, we tentatively identified as ellagic acid galloyl hexoside [53].

Docking upon urease

Quercetin 3-O-(6''-galloyl)-β-D-galactopyranoside interacted with three of the critical residues of urease active site, namely Asp633, Cme 592, and Arg439, forming one conventional H bond with Asp633, and one Sulfur H bond with Cme592 (Figure 6). Also, a pi-cation interaction between Arg609 and the A-ring aromatic system is observed. In detail, the hydroxyl group in C-7 can chelate with two nickel ions (Ni 901, Ni 902) and acted as an H acceptor to form hydrogen bonding with Asp 633. Furthermore, hydrophobic (Pi-alkyl) interaction was established between A and C rings with Ala 636. On the other hand, one-carbon H bond, and pi-alkyl with Arg439. Apart from these residues, it has also interacted with Ala636, forming one pi-sigma bond and one pi-alkyl bond. Therefore, this compound was able to locate deeply in the enzyme active site, generating a binding energy of −7.9 kcal/mol with a IC50 value of 1.62 µM (Figure 6).

Microscale thermophoresis (MST) study of the interaction between quercetin 3-O-(6''-galloyl)-β-D-galactopyranoside and Jack bean urease.

Microscale thermophoresis (MST) is a biophysical technique used to investigate bio-molecular interaction. This technique allows to determine the strength of the interaction between two molecules by detecting variations in the fluorescence signal because of an IR laser-induced temperature change [54].

The magnitude of the fluorescence change (Figure7) correlates with the binding (complex) of a ligand to the fluorescent target [55,56]. In our laboratory used Label-Free MST, which is based on the movement of a native protein within a temperature gradient. So, the fluorescence peak signal corresponds to the innate florescence of the target protein due to tyrosine (Tyr), tryptophan (Trp), and phenylalanine (Phe) residues. Label-free MST also has broad applications for lipid and RNA/DNA interaction.

Concentrations ranging from picomolar to molar with little sample consumption and no immobilization of the protein of interest are the main advantages of this technique [57]. In our experiment, the interaction between the flavonoid and urease is evident, although an aggregation phenomenon is observed that prevents progress towards the exact determination of the affinity constant. The aggregation is not due to adhesion of the protein to the capillaries since it used premium coated capillary and pluoronic.

Figure 7. Complex formation between ligand quercetin 3-O-(6''-galloyl)-β-D-galactopyranoside and target protein (Jack bean urease).

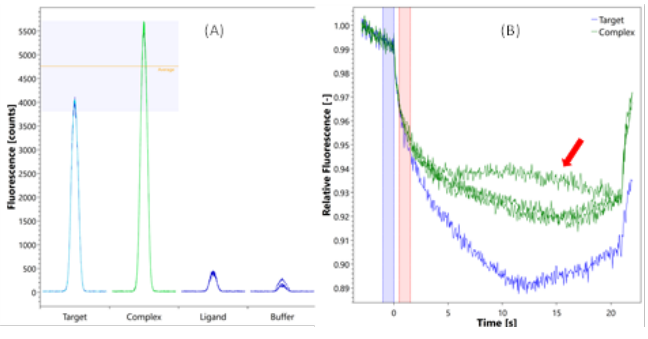

(A) Fluorescence of target urease, complex enzyme-ligand, ligand, and buffer alone. (B). Unlabeled urease in PBS + without (blue curve) and with 1 mM compound (green curve). Cold (blue) and hot (red) regions as defined in central data analysis to calculate $_{Frelat}$. Arrowhead point to protein aggregation.

The aggregation phenomena are evidenced by splitting of the fluorescence peaks, so in our experiment the aggregation of urease seems to be spontaneous and increases in the presence of the ligand. In the Figure 7 it is observed the ligand-induced aberrant MST traces due to protein aggregation/denaturation at elevated ligand concentration. Red arrows highlight aberrant MST traces. Focusing on the mechanisms of aggregation induced by physical instabilities, both colloidal and conformational changes are described to potentially promote aggregation. Whereas for colloidal interactions, changes in certain properties of the solvent such as pH and salt concentration could alter charge of the protein leading to association between structurally native molecules. Such conformational changes modify the native structure, thereby generating folding-intermediates that are prone to aggregation [58].

Therefore, there is two forms of aggregation: native aggregation and non-native aggregation, depending on the structural integrity of the protein involved. Native aggregation normally is a reversible process, while non-native aggregation often leads to irreversible aggregate. Given that there are no previous studies evaluating the interaction of small molecules with urease using MST, it is a future challenge to find the set of measurement parameters that allow this technology to be used for the discovery of new inhibitors.

CONCLUSIONS

In this work, the antimicrobial activity of UMAE, a plant used in traditional Chilean medicine, has been evaluated. Among its antimicrobial properties, the effect on *H. pylori* stands out, and is especially its ability to inhibit urease, a crucial enzyme for the survival of this pathogen. Using a workflow that considered the micro-fractionation of the extract coupled to a high-throughput urease assay, the most relevant fractions were identified.
Subsequently, active fraction was separated by centrifugal partition chromatography (CPC) and using the off-line urease assay in parallel with the HPLC MS/MS analysis, it was possible to identify that the inhibitory compounds correspond to quercetin galloyl hexosides. Molecular docking and biomolecular interaction experiments by MST corroborate our findings. In general, this article reports for the first time an activity of *U. molinae* that supports its gastroprotective effects and adds new therapeutic qualities to this interesting native plant resource.

ACKNOWLEDGMENTS

This work was supported by a regular project (#1211119) from FONDECYT, and FONDEQUIP EQM200098 from ANID, the Chilean National Research and Development Agency.

REFERENCES

1. López, J.; Vega-Gálvez, A.; Rodríguez, A.; Uribe, E.; Bilbao-Sainz, C. Review MURTA (Ugni Molinae Turcz.): A Review on Chemical Composition, Functional Components and Biological Activities of Leaves and Fruits. *Chilean J. Agric. Anim. Sci., ex Agro-Ciencia* 2018.
2. Schreckinger, M.E.; Lotton, J.; Lila, M.A.; de Mejia, E.G. Berries from South America: A Comprehensive Review on Chemistry, Health Potential, and Commercialization. *J Med Food* 2010.
3. Alfaro, S.; Mutis, A.; Palma, R.; Quiroz, A.; Seguel, I.; Scheuermann, E. Influence of Genotype and Harvest Year on Polyphenol Content and Antioxidant Activity in Murtilla (Ugni Molinae Turcz) Fruit. *J Soil Sci Plant Nutr* 2013.
4. Peña-Cerda, M.; Arancibia-Radich, J.; Valenzuela-Bustamante, P.; Pérez-Arancibia, R.; Barriga, A.; Seguel, I.; García, L.; Delporte, C. Phenolic Composition and Antioxidant Capacity of Ugni Molinae Turcz. Leaves of Different Genotypes. *Food Chem* 2017.
5. Avello Lorca, M.; Pastene Navarrete, E.; Barriga, A.; Bittner Berner, M.; Ruiz Ponce, E.; Becerra Allende, J. Chemical Properties and Assessment of the Antioxidant Capacity of Native Species from the Genus Ugni. *Revista Cubana de Plantas Medicinales* 2016.
6. Avello Lorca, M.; Pastene Navarrete, E.; González Riquelme, M.; Bittner Berner, M.; Becerra Allende, J. In Vitro Determination of the Antioxidant Capacity of Extracts and Phenolic Compounds from Ugni Molinae Turcz. Leaves. *Revista Cubana de Plantas Medicinales* 2013.
7. Avello, M.; Torres, E.; Carvajal, R.I.; Pastene, E. Effect of in Vitro Digestion Gastrointestinal of the Extract Aqueou of Leaves of Ugni Molinae, on the Viability of Colorectal Cancer Cells. *Journal of the Chilean Chemical Society* 2021.
8. Torres Vallejos, E.; Avello, M.; Pastene, E. Identification of Water-Soluble Compounds Contained in Aqueos Extracts and Fractions Obtained from Leaves of Ugni Molinae to Determine Their Effect on the Viability of Humna Gastric Cancer Cells. *Journal of the Chilean Chemical Society;* Vol 65 No 2 (2020).
9. Jara-Moreno, D.; Riveros, A.L.; Barriga, A.; Kogan, M.J.; Delporte, C. Inhibition of β-Amyloid Aggregation of Ugni Molinae Extracts. *Curr Pharm Des* 2020.
10. Pérez-Arancibia, R.; Ordoñez, J.L.; Rivas, A.; Pihán, P.; Sagredo, A.; Ahumada, U.; Barriga, A.; Seguel, I.; Cárdenas, C.; Vidal, R.L.; et al. A Phenolic-Rich Extract from Ugni Molinae Berries Reduces Abnormal Protein Aggregation in a Cellular Model of Huntington's Disease. *PLoS One* 2021.
11. Makarewicz, M.; Drożdż, I.; Tarko, T.; Duda-Chodak, A. The Interactions between Polyphenols and Microorganisms, Especially Gut Microbiota. *Antioxidants* 2021.
12. Piwowarski, J.P.; Granica, S.; Stefańska, J.; Kiss, A.K. Differences in Metabolism of Ellagitannins by Human Gut Microbiota Ex Vivo Cultures. *J Nat Prod* 2016.

13. Luo, C.; Wei, X.; Song, J.; Xu, X.; Huang, H.; Fan, S.; Zhang, D.; Han, L.; Lin, J. Interactions between Gut Microbiota and Polyphenols: New Insights into the Treatment of Fatigue. *Molecules* 2022.
14. Cires, M.J.; Wong, X.; Carrasco-Pozo, C.; Gotteland, M. The Gastrointestinal Tract as a Key Target Organ for the Health-Promoting Effects of Dietary Proanthocyanidins. *Front Nutr* 2017.
15. Andriamihaja, M.; Lan, A.; Beaumont, M.; Grauso, M.; Gotteland, M.; Pastene, E.; Cires, M.J.; Carrasco-Pozo, C.; Tomé, D.; Blachier, F. Proanthocyanidin-Containing Polyphenol Extracts from Fruits Prevent the Inhibitory Effect of Hydrogen Sulfide on Human Colonocyte Oxygen Consumption. *Amino Acids* 2018.
16. Cires, M.J.; Navarrete, P.; Pastene, E.; Carrasco-Pozo, C.; Valenzuela, R.; Medina, D.A.; Andriamihaja, M.; Beaumont, M.; Blachier, F.; Gotteland, M. Protective Effect of an Avocado Peel Polyphenolic Extract Rich in Proanthocyanidins on the Alterations of Colonic Homeostasis Induced by a High-Protein Diet. *J Agric Food Chem* 2019.
17. Cires, M.J.; Navarrete, P.; Pastene, E.; Carrasco-Pozo, C.; Valenzuela, R.; Medina, D.A.; Andriamihaja, M.; Beaumont, M.; Blachier, F.; Gotteland, M. Effect of a Proanthocyanidin-Rich Polyphenol Extract from Avocado on the Production of Amino Acid-Derived Bacterial Metabolites and the Microbiota Composition in Rats Fed a High-Protein Diet. *Food Funct* 2019.
18. Wong, X.; Carrasco-Pozo, C.; Escobar, E.; Navarrete, P.; Blachier, F.; Andriamihaja, M.; Lan, A.; Tomé, D.; Cires, M.J.; Pastene, E.; et al. Deleterious Effect of P-Cresol on Human Colonic Epithelial Cells Prevented by Proanthocyanidin-Containing Polyphenol Extracts from Fruits and Proanthocyanidin Bacterial Metabolites. *J Agric Food Chem* 2016.
19. Wang, X.; Qi, Y.; Zheng, H. Dietary Polyphenol, Gut Microbiota, and Health Benefits. Antioxidants 2022, 11.
20. Medicinales Aromáticas, P. *Boletín Latinoamericano y Del Caribe De*. 2009.
21. Malfertheiner, P.; Megraud, F.; O'Morain, C.; Gisbert, J.P.; Kuipers, E.J.; Axon, A.; Bazzoli, F.; Gasbarrini, A.; Atherton, J.; Graham, D.Y.; et al. Management of Helicobacter Pylori Infection-the Maastricht V/Florence Consensus Report. *Gut* 2017.
22. Kusters, J.G.; Kuipers, E.J. Antibiotic Resistance of Helicobacter Pylori. *J Appl Microbiol* 2001.
23. Sachs, G.; Scott, D.R. Helicobacter Pylori: Eradication or Preservation. *F1000 Med Rep* 2012.
24. Mobley, H.L.T.; Hu, L.T.; Foxall, P.A. Helicobacter Pylori Urease: Properties and Role in Pathogenesis. *Scand J Gastroenterol* 1991.
25. Malfertheiner, P.; Camargo, M.C.; El-Omar, E.; Liou, J.M.; Peek, R.; Schulz, C.; Smith, S.I.; Suerbaum, S. Helicobacter Pylori Infection. *Nat Rev Dis Primers* 2023.
26. Wroblewski, L.E.; Peek, R.M.; Wilson, K.T. Helicobacter Pylori and Gastric Cancer: Factors That Modulate Disease Risk. *Clin Microbiol Rev* 2010.
27. Ferreccio, C.; Rollán, A.; Harris, P.R.; Serrano, C.; Gederlini, A.; Margozzini, P.; Gonzalez, C.; Aguilera, X.; Venegas, A.; Jara, A. Gastric Cancer Is Related to Early Helicobacter Pylori Infection in a High-Prevalence Country. *Cancer Epidemiology Biomarkers and Prevention* 2007.
28. Roesler, B.M.; Botelho Costa, S.C.; Murilo, J.; Zeitune, R. Eradication Treatment of Helicobacter Pylori Infection: Its Importance and Possible Relationship in Preventing the Development of Gastric Cancer. *International Scholarly Research Network ISRN Gastroenterology* 2012.
29. Ambrosi, C.; Sarshar, M.; Aprea, M.R.; Pompilio, A.; Di Bonaventura, G.; Strati, F.; Pronio, A.; Nicoletti, M.; Zagaglia, C.; Palamara, A.T.; et al. Colonic Adenoma-Associated Escherichia Coli Express Specific Phenotypes. *Microbes Infect* 2019.
30. Williams, M.A.; Schmidt, R.L.; Lenz, L.L. Early Events Regulating Immunity and Pathogenesis during Listeria Monocytogenes Infection. *Trends Immunol* 2012.
31. Flickinger, J.C.; Rodeck, U.; Snook, A.E. Listeria Monocytogenes as a Vector for Cancer Immunotherapy: Current Understanding and Progress. *Vaccines (Basel)* 2018.
32. Castro-Seriche, S.; Jerez-Morales, A.; Smith, C.T.; Sánchez-Alonzo, K.; García-Cancino, A. Candida Albicans, a Reservoir of Listeria Monocytogenes? Infection, *Genetics and Evolution* 2021.
33. Santativongchai, P.; Tulayakul, P.; Jeon, B. Enhancement of the Antibiofilm Activity of Nisin against Listeria Monocytogenes Using Food Plant Extracts. *Pathogens* 2023.
34. Liu, F.; Rajabi, S.; Shi, C.; Afifirad, G.; Omidi, N.; Kouhsari, E.; Khoshnood, S.; Azizian, K. Antibacterial Activity of Recently Approved Antibiotics against Methicillin-Resistant Staphylococcus Aureus (MRSA) Strains: A Systematic Review and Meta-Analysis. *Ann Clin Microbiol Antimicrob* 2022.
35. Cascioferro, S.; Carbone, D.; Parrino, B.; Pecoraro, C.; Giovannetti, E.; Cirrincione, G.; Diana, P. Therapeutic Stra-tegies To Counteract Antibiotic Resistance in MRSA Biofilm-Associated Infections. *ChemMedChem* 2021.
36. Ejaz, M.; Syed, M.A.; Jackson, C.R.; Sharif, M.; Faryal, R. Epidemiology of Staphylococcus Aureus Non-Susceptible to Vancomycin in South Asia. *Antibiotics* 2023.
37. Jajere, S.M. A Review of Salmonella Enterica with Particular Focus on the Pathogenicity and Virulence Factors, Host Specificity and Antimicrobial Resistance Including Multidrug Resistance. *Vet World* 2019.
38. Hendriksen, S.W.M.; Orsel, K.; Wagenaar, J.A.; Miko, A.; van Duijkeren, E. Animal-to-Human Transmission of Salmonella Typhimurium DT104A Variant. *Emerg Infect Dis* 2004.
39. Hebel-Gerber, S.; García-Cancino, A.; Urbina, A.; Simirgiotis, M.J.; Echeverría, J.; Bustamante-Salazar, L.; Sáez-Carrillo, K.; Alarcón, J.; Pastene-Navarrete, E. Chilean Rhubarb, Gunnera Tinctoria (Molina) Mirb. (Gunneraceae): UHPLC-ESI-Orbitrap-MS Profiling of Aqueous Extract and Its Anti-Helicobacter Pylori Activity. *Front Pharmacol* 2021.

40.Chávez, F.; Aranda, M.; García, A.; Pastene, E. Antioxidant Polyphenols Extracted from Avocado Epicarp (Persea Americana Var. Hass) Inhibit Helicobacter Pylori Urease. *Bol Latinoam Caribe Plantas Med Aromat* 2011.

41. Pastene, E.; Troncoso, M.; Figueroa, G.; Alarcón, J.; Speisky, H. Association between Polymerization Degree of Apple Peel Polyphenols and Inhibition of Helicobacter Pylori Urease. *J Agric Food Chem* 2009.

42.Pastene, E.; Parada, V.; Avello, M.; Ruiz, A.; García, A. Catechin-Based Procyanidins from Peumus Boldus Mol. Aqueous Extract Inhibit Helicobacter Pylori Urease and Adherence to Adenocarcinoma Gastric Cells. *Phytotherapy Research* 2014.

43. Linke, P.; Amaning, K.; Maschberger, M.; Vallee, F.; Steier, V.; Baaske, P.; Duhr, S.; Breitsprecher, D.; Rak, A. An Automated Microscale Thermophoresis Screening Approach for Fragment-Based Lead Discovery. *J Biomol Screen* 2016.

44.Ribeiro, M.L.; Gerrits, M.M.; Benvengo, Y.H.B.; Berning, M.; Godoy, A.P.O.; Kuipers, E.J.; Mendonça, S.; Van Vliet, A.H.M.; Pedrazzoli, J.; Kusters, J.G. Detection of High-Level Tetracycline Resistance in Clinical Isolates of Helicobacter Pylori Using PCR-RFLP. *FEMS Immunol Med Microbiol* 2004.

45. Grossman, T.H. Tetracycline Antibiotics and Resistance. *Cold Spring Harb Perspect Med.*2016.

46.Mroczek, T.; Dymek, A.; Widelski, J.; Wojtanowski, K.K. The Bioassay-Guided Fractionation and Identification of Potent Acetylcholinesterase Inhibitors from Narcissus c.v. 'Hawera' Using Optimized Vacuum Liquid Chromatography, High Resolution Mass Spectrometry and Bioautography. *Metabolites* 2020.

47. McCallum, J.L.; Vacon, J.N.D.; Kirby, C.W. Ultra-Micro-Scale-Fractionation (UMSF) as a Powerful Tool for Bioactive Molecules Discovery. *Molecules* 2020.

48.Wang, R.; Liu, Y.; Zhou, H.; Chen, Y.; Wang, J.; Zhang, X.; Yu, R.; Liang, X. Integration of Micro-Fractionation, High-Performance Liquid Chromatography-Ultraviolet Detector-Charged Aerosol Detector-Mass Spectrometry Analysis and Cellular Dynamic Mass Redistribution Assay to Accelerate Alkaloid Drug Discovery. *J Chromatogr A*. 2020.

49. Krajewska, B.; Van Eldik, R.; Brindell, M. Temperature- and Pressure-Dependent Stopped-Flow Kinetic Studies of Jack Bean Urease. Implications for the Catalytic Mechanism. *Proceedings of the Journal of Biological Inorganic Chemistry;* 2012.

50. Weatherburn, M.W.; Lubochinsky, B.; Zalta, J.P.; St, B. Phenol-Hypochlorite Reaction for Determination of Ammonia; *UTC*, 1954.

51. Ito, Y. Golden Rules and Pitfalls in Selecting Optimum Conditions for High-Speed Counter-Current Chromatography. J *Chromatogr A* 2005.

52.Hubert, J.; Plé, K.; Hamzaoui, M.; Renault, J.H. *Polyphenol Purification by Solid Support-Free Liquid—Liquid Chromatography (CCC, CPC).* In Natural Products: Phytochemistry, Botany and Metabolism of Alkaloids, Phenolics and Terpenes; Springer Berlin Heidelberg, 2013.

53. Xu, M.; Liu, P.; Jia, X.; Zhai, M.; Zhou, S.; Wu, B.; Guo, Z. Metabolic Profiling Revealed the Organ-specific Distribution Differences of Tannins and Flavonols in Pecan. *Food Sci Nutr* 2020.

54. Rainard, J.M.; Pandarakalam, G.C.; McElroy, S.P. Using Microscale Thermophoresis to Characterize Hits from High-Throughput Screening: A European Lead Factory Perspective. *SLAS Discovery* 2018, 23, 225–241.

55. Nasreddine, R.; Nehmé, R. Microscale Thermophoresis for Studying Protein-Small Molecule Affinity: Application to Hyaluronidase. *Microchemical Journal* 2021

56. Hellinen, L.; Bahrpeyma, S.; Rimpelä, A.K.; Hagström, M.; Reinisalo, M.; Urtti, A. Microscale Thermophoresis as a Screening Tool to Predict Melanin Binding of Drugs. *Pharmaceutics*. 2020.

57. Asmari, M.; Ratih, R.; Alhazmi, H.A.; El Deeb, S. Thermophoresis for Characterizing Biomolecular Interaction. *Methods*.2018.

58. Wang, W. Protein Aggregation and Its Inhibition in Biopharmaceutics. *Int J Pharm* 2005.